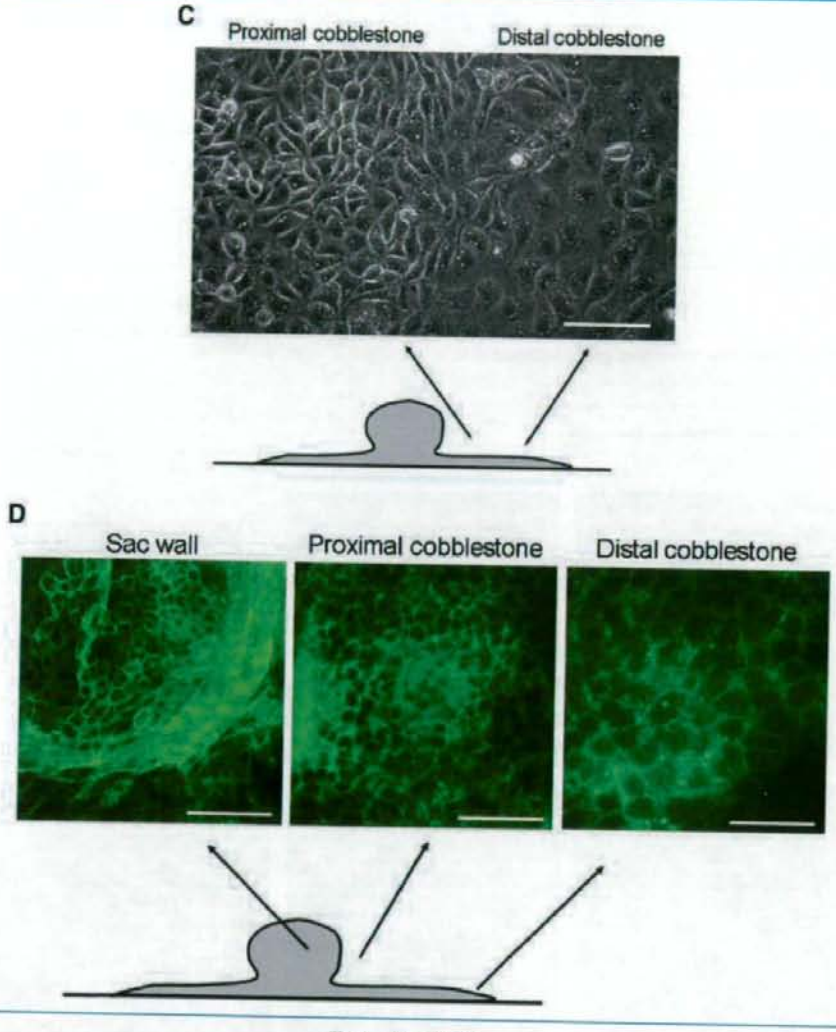

Fig. 1. (*Continued*)

VEGF-R3, a marker for lymphatic endothelial and embryonic vascular endothelial cells, was detected at fairly high levels in cmES-derived cells and HUVEC. The expression of VEGF-R2, a marker for vascular and lymphatic endothelial cells, was constantly detected at the same level as VE-cadherin, as we confirm it by detailed analyses in the following part of the manuscript (Fig. 5). From these flow cytometric analyses, it was concluded that cmES-derived cells resembled HUVEC rather than HAEC.

Although limited populations of cmES-derived cells were positive for cell surface VE-cadherin/PECAM-1, their uniform Ac-LDL-uptaking activities and uniform expressions of eNOS and vWF, taken together with their cord-forming activities and VEGF-R1 expression equivalent to HUVEC, suggest that the almost all of the cmES-derived cells are vascular endothelial cells or vascular endothelial endothelial-like cells and, therefore, "VE-cadherin/PECAM-1-negative" populations are also types of cells that are closely related to the vascular endothelial cells. This idea was analogous to the proposal by Thomson and colleagues (Kaufman et al., 2004). They showed that rmES-derived vascular endothelial cells were negative for VE-cadherin/PECAM-1 despite the presence of mature endothelial functions with eNOS and vWF expressions. They used commercially available EGM™-2 BulletKit for the differentiation of rmES cells. Eventually, usage of EGM™-2 BulletKit resulted in the production of almost pure VE-cadherin/PECAM-1-negative vascular endothelial cells by our method as the report by Thomson and colleagues. As shown in Figure 4, differentiation induction by our method using EGM™-2 BulletKit resulted in generation of cells with mature

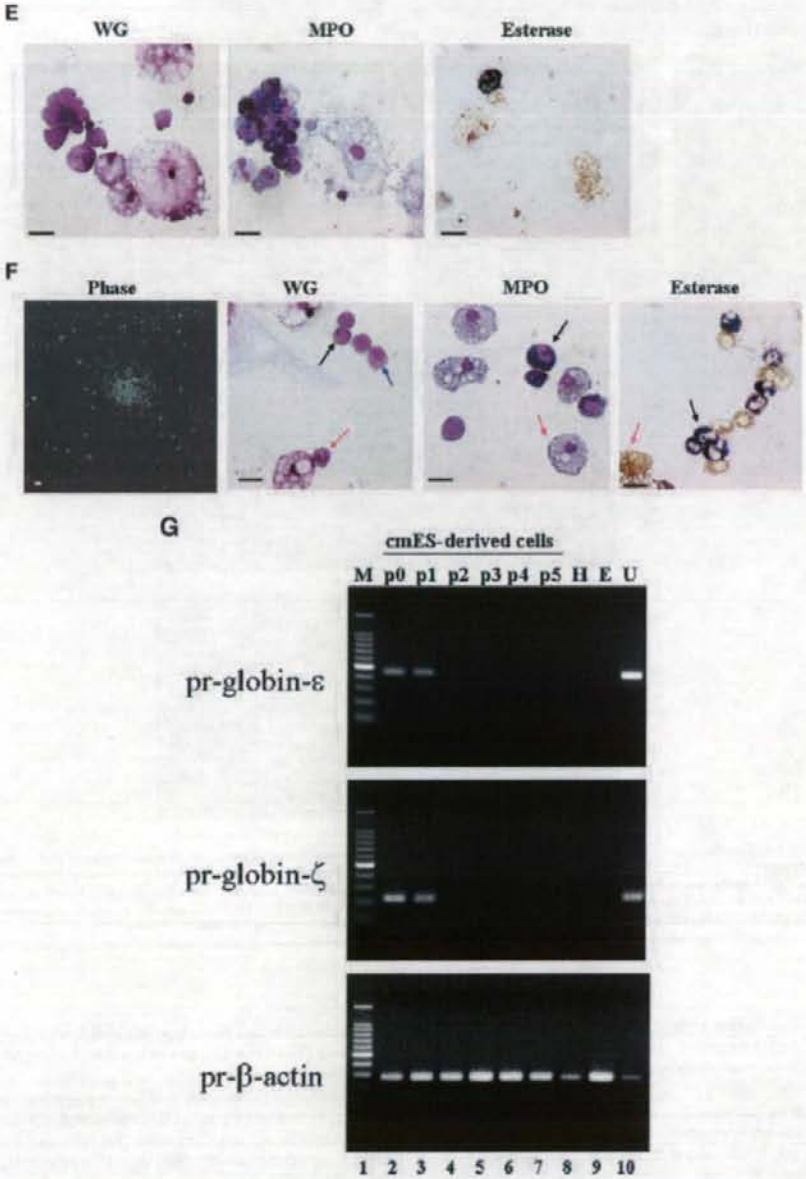

Fig. 1. (*Continued*)

functions including cord-forming activities (Fig. 4A, upper right in EGM2 part) and uniform Ac-LDL-uptaking activities (Fig. 4A, middle and lower right in EGM2 part) and with eNOS and vWF expressions (Fig. 4B, EGM2 part) despite the lack of VE-cadherin/PECAM-1 as assessed by flow cytometry (Fig. 4A, lower left in EGM2 part). In contrast to the findings by Thomson and colleagues (Kaufman et al., 2004), VE-cadherin expression was detected by Western blotting (Fig. 4C) in our culture system even by using EGM®-2 BulletKit, indicating that VE-cadherin protein was really produced though its membrane translocation seems to be blocked by unknown reason(s). Anyway, it can be concluded that there existed an "atypical"

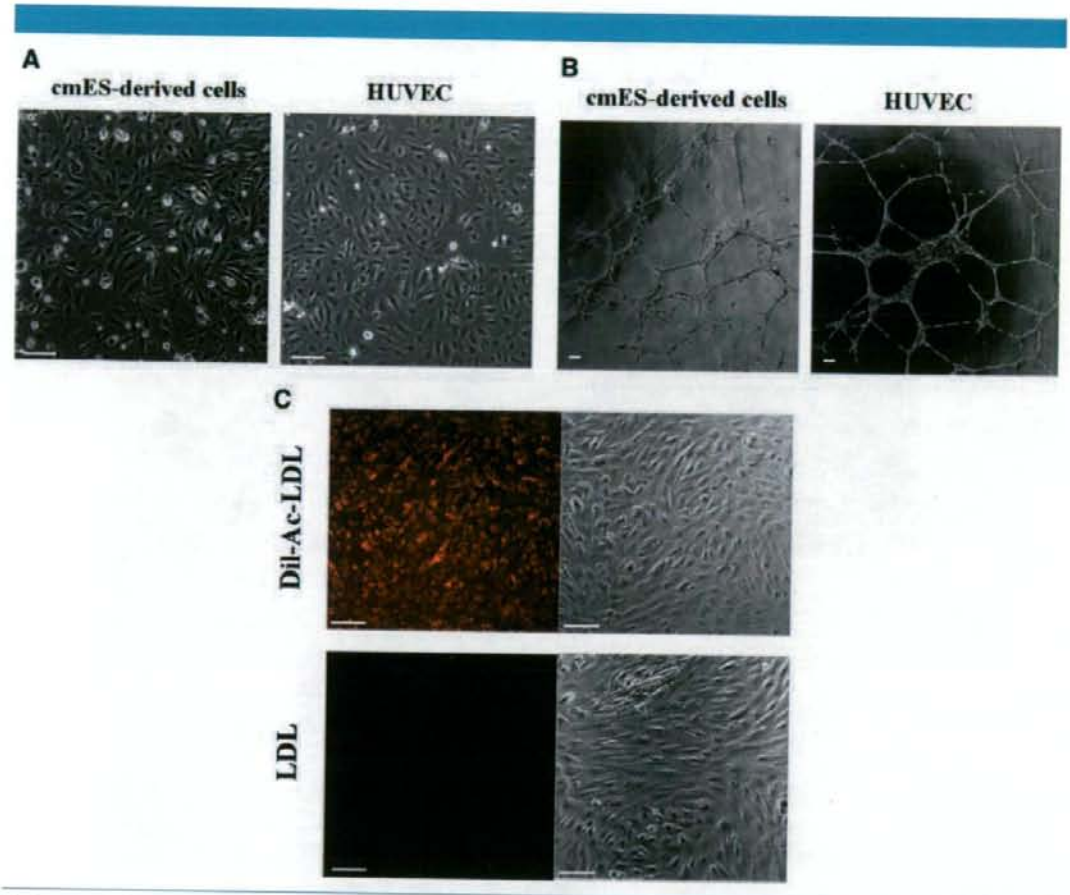

Fig. 2. Morphology and functions of cmES-derived subcultured cells. A: The phase contrast microscopy. Morphologies of cmES-derived cells (left) and HUVEC (right) were shown. The scale bar indicates 100 μm. B: Cord formation assays. A cord-forming activity of cmES-derived cells (left) and HUVEC (right) was shown. The scale bar indicates 100 μm. C: Ac-LDL-uptaking assays. Fluorescence (DiI)-labeled Ac-LDL (upper) or non-labeled LDL (lower) was added to cmES-derived cells. After overnight culture, cells were observed under fluorescence microscopy. Right parts indicate the photographs with Normarsky differentiated interference contrast. The scale bar indicates 20 μm.

type of vascular endothelial cells (i.e., cell surface VE-cadherin/PECAM-1-negative vascular endothelial cells) among primate ES-derived differentiated cells.

For further understanding of cell surface VE-cadherin-positive "canonical" vascular endothelial cells and cell surface VE-cadherin-negative "atypical" vascular endothelial cells, we fractionated those two populations by FACSAria. As shown in Figure 5C, cell surface VE-cadherin-positive populations proliferated as VE-cadherin-positive cells and expanded by 160-fold after five passages. Interestingly, cell surface VE-cadherin-positive populations were positive for cell surface CD34 expression as assessed by flow cytometry (Fig. 5D). The immunostaining study of cell surface VE-cadherin-positive cells clearly showed the localization of VE-cadherin at intercellular junctions in these cells (Fig. 5E). The functional maturation including cord-forming activities (Fig. 5F) and uniform Ac-LDL-uptaking activities (Fig. 5G) was also detected in cell surface VE-cadherin-positive populations. Expressions of other vascular endothelial markers were also detected including VEGF-R1, VEGF-R2, VEGF-R3, and Tie-2 (Fig. 5H). On the other hand, the cell surface VE-cadherin-negative populations proliferated as VE-cadherin-negative cells and were negative for cell surface CD34 expression (Fig. 6A–D). Interestingly, these cells showed obvious cord-forming capacities (Fig. 6E) and a uniform Ac-LDL-uptaking activity (Fig. 6F). Moreover, they expressed VEGF-R1, VEGF-R3, and Tie-2 despite the absence of VEGF-R2 as demonstrated by flow cytometric analyses (Fig. 6G). Immunostaining studies using an anti-VE-cadherin antibody demonstrated intracellular region-staining patterns (Fig. 6H), suggesting that the cell surface VE-cadherin-negative cells expressed VE-cadherin intracellularily. This finding was confirmed by Western blotting studies, which showed the presence of the 130-kDa VE-cadherin band (Fig. 6I). RT-PCR studies further demonstrated the presence of the VE-cadherin message (Fig. 6J). As monocytes/macrophages or other hematopoietic cells reportedly show various endothelial cell-like features and are positive for VEGF-R1 and VEGF-R3

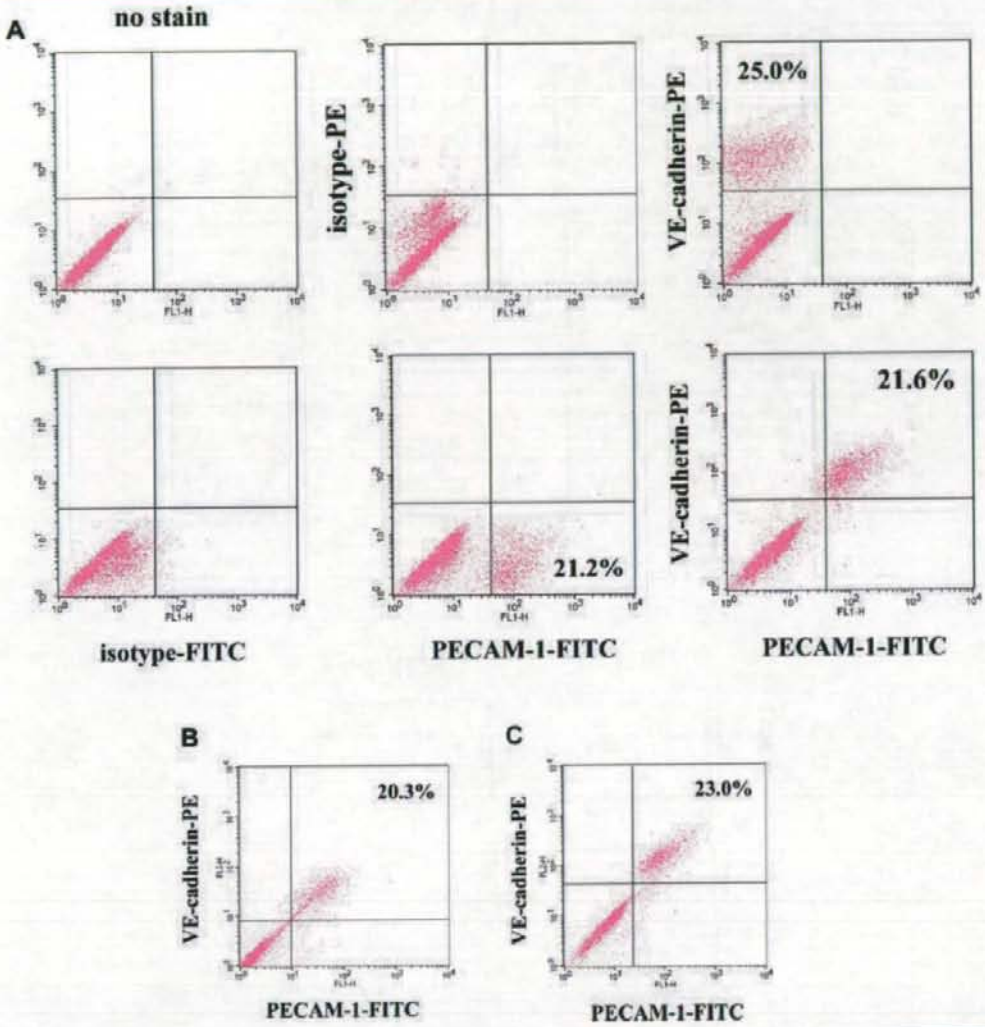

Fig. 3. Cell surface expressions of vascular endothelial markers in cmES-derived subcultured cells. A–C: Cell surface expressions of VE-cadherin and PECAM-1. The total adherent cells obtained by culture of cmES-derived spheres on gelatin-coated plates were subcultured and, after six passages (A) or eight passages (B), cells were stained by a PE-labeled anti-human VE-cadherin antibody (vertical axes), a FITC-labeled anti-human PECAM-1 antibody (horizontal axes) or each isotype control antibody as indicated. C: The total adherent cells obtained by the culture of cmES-derived spheres on gelatin-coated plates were frozen. After being thawed, cells were cultured for additional two passages and the expressions of VE-cadherin and PECAM-1 were determined by flow cytometry as in (A). D: Expressions of other endothelial markers. cmES-derived cells (ESdC), HUVEC and HAEC were subjected to flow cytometric analyses using indicated monoclonal antibodies.

(Fernandez Pujol et al., 2001; Kuwana et al., 2006), we examined the expressions of monocyte/macrophage markers of CD68, CD14 and CD11b as well as pan-leukocyte markers of CD18 and CD45. We found that the cell surface VE-cadherin-negative populations were negative for CD68 (Fig. 6K), CD14 (Fig. 6L), CD11b (Fig. 6L), CD18 (Fig. 6L), and CD45 (Fig. 6L), indicating that they are distinct from hematopoietic endothelial cell progenitors.

All those findings together suggest that our differentiation system produced almost two pure populations: cell surface VE-cadherin-positive "canonical" vascular endothelial cells and cell surface VE-cadherin-negative "atypical" vascular endothelial cells. This concept was further confirmed by the fact that neither pericytes nor undifferentiated ES cells co-existed in the differentiated samples. Pericytes are reportedly induced during vascular endothelial differentiation (Yamashita et al., 2000; Sone et al., 2003, 2007). Moreover, co-existence of pericytes, the polygonal cells, severely inhibits the expansion of vascular endothelial cells during subculture (Sone et al., 2003, 2007). In our system, however, both

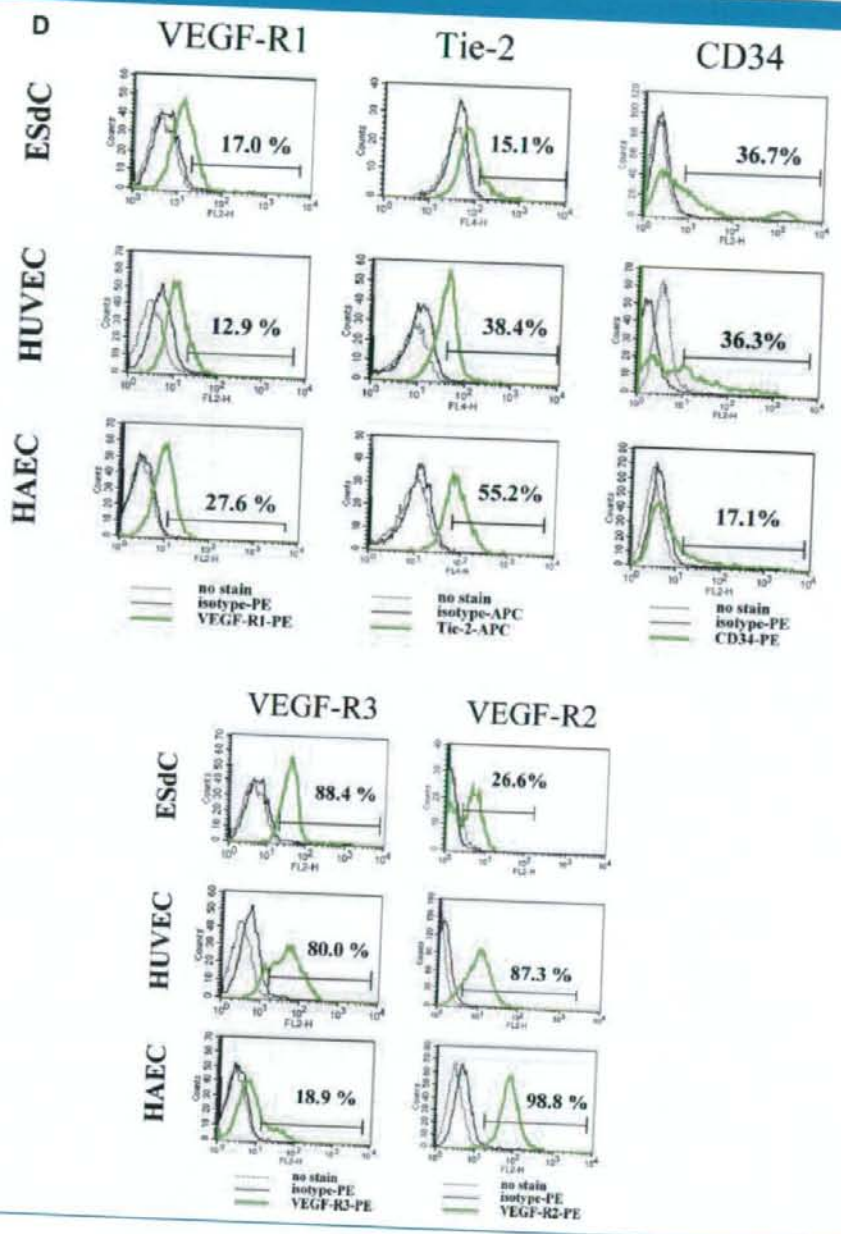

Fig. 3. *(Continued)*

VE-cadherin-positive and VE-cadherin-negative populations showed quite similar spindle-shaped morphologies (but not polygonal shape) and were undistinguishable by microscopic observations (Figs. 5B and 6B). Indeed, our differentiated samples were negative for the expressions of smooth muscle actin (SMA)-α, a marker for smooth muscle cells, and PDGF receptor β, a marker for pericytes (Fig. 7A). As shown in Figure 7B,C, Nanog expression was not detected in ES-derived cells, excluding the possible existence of undifferentiated ES cells. Finally, genomic PCR studies excluded the contamination of MEFs, which were used only in the maintenance culture of undifferentiated cmES cells (Fig. 7D).

Thus, our novel method has enabled the highest efficiency vascular endothelial differentiation from primate ES cells,

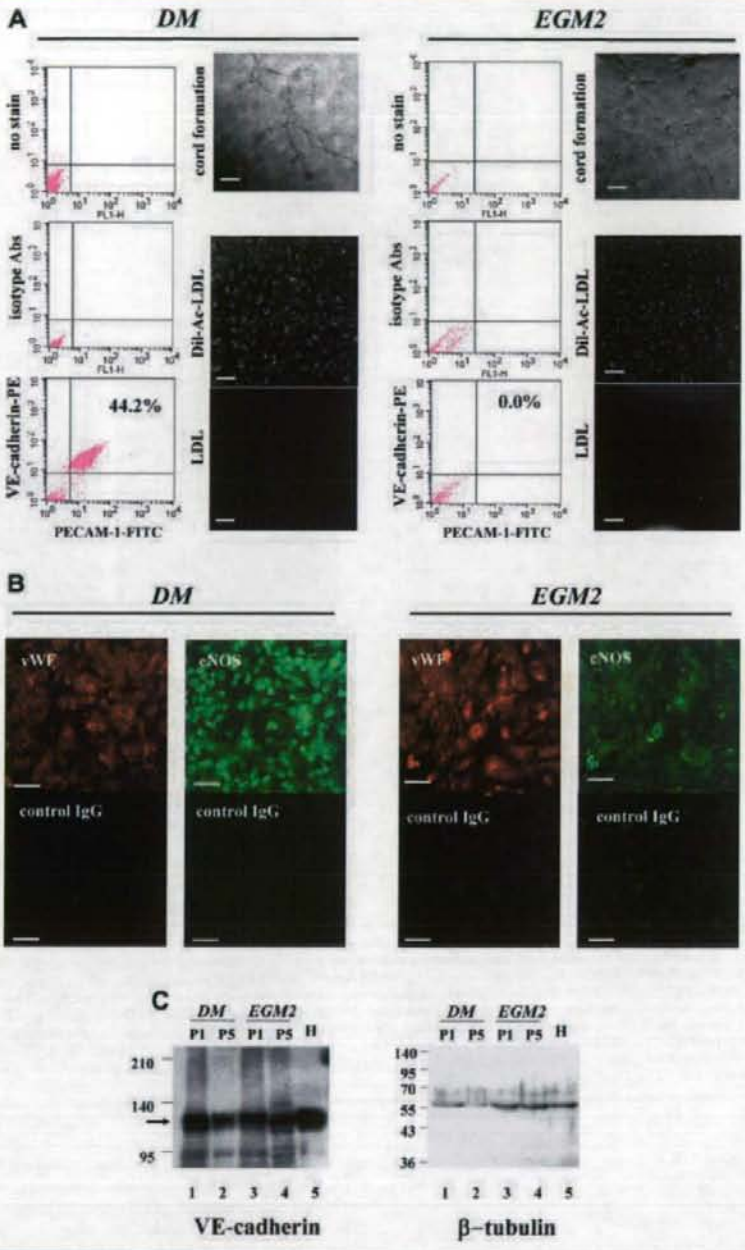

Fig. 4. Generation of atypical vascular endothelial cells by using commercially available culture medium. Differentiation procedure was performed either by using the differentiation medium supplemented with six cytokines (*DM*) or EGM™-2 BulletKit medium (*EGM2*). A: After two passages, flow cytometric analyses for cell surface VE-cadherin/PECAM-1 expressions (left parts), cord formation assays (right upper parts) and Ac-LDL uptaking assays (right lower parts) were performed in each culture condition (DM culture or EGM2 culture). The scale bar indicates 100 μm. B: After two passages, cells were fixed and stained by an anti-human vWF goat polyclonal antibody (red) and an anti-human eNOS rabbit polyclonal antibody (green). The scale bar indicates 50 μm. Similar results were obtained at passage number at least up to 7 (data not shown). C: At indicated numbers of passage, cells were collected and Western blotting was performed using an anti-human VE-cadherin rabbit polyclonal antibody. Arrows indicate the 130 kDa VE-cadherin protein (left part). For positive control, HUVEC lysate was used (lane 5, "H"). For internal control, β-tubulin expressions were determined (right part).

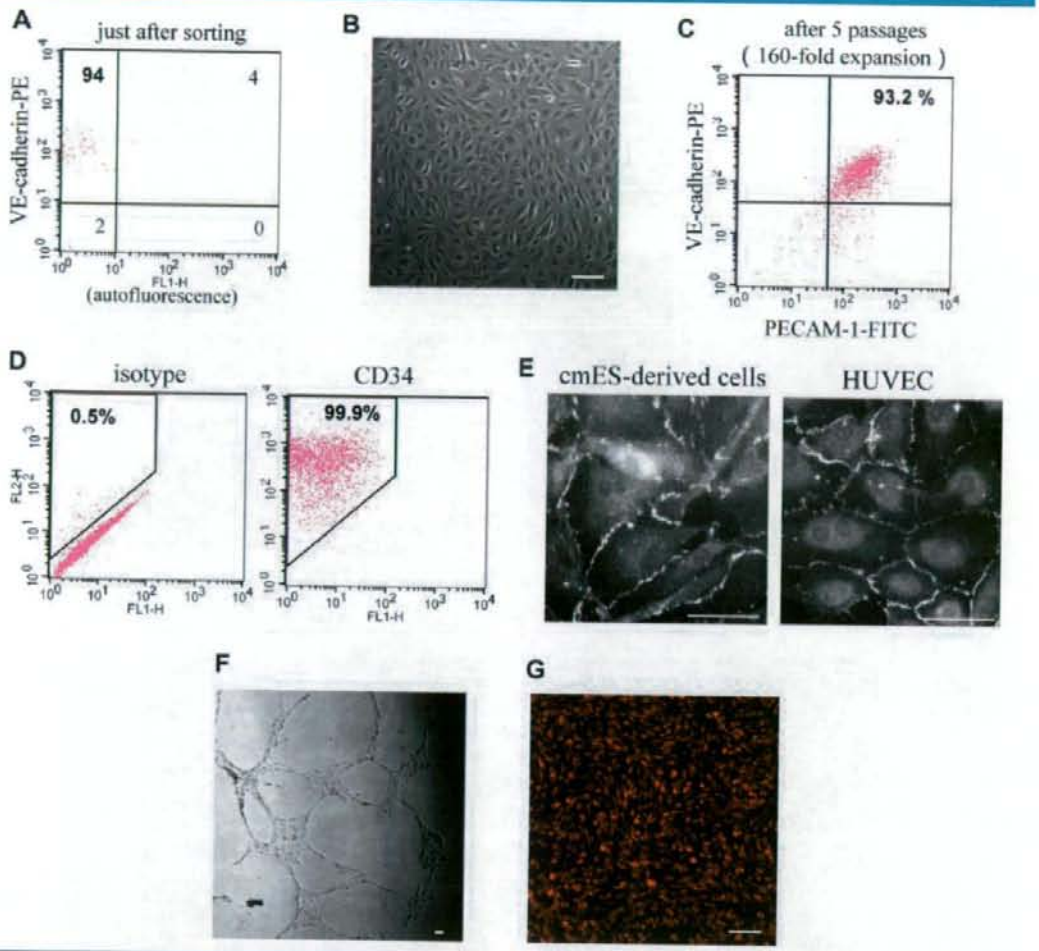

Fig. 5. Expansion and characterization of cell surface VE-cadherin-positive populations. Differentiation procedure was performed, and after the first passage, cell surface VE-cadherin-positive fraction was sorted by FACSAria™. A: The expression of VE-cadherin was determined just after sorting. B: After a few days culture, cell morphology was observed under an inverted phase contrast light microscope. The scale bar indicates 100 μm. C: After five passages, the cell surface expressions of VE-cadherin/PECAM-1 were re-studied by flow cytometry. D: The cell surface expression of CD34 was also studied by flow cytometry. E: Localization of VE-cadherin at intercellular junctions was confirmed by immunostaining using HUVEC as positive control. The scale bar indicates 50 μm. F,G: The functional analyses. Cord-forming activities (F) and Ac-LDL-uptaking capacities (G) were confirmed. The scale bar indicates 100 μm. H: Cell surface expressions of other endothelial markers (VEGF-R2, VEGF-R1, VEGF-R3, and Tie-2) were studied by flow cytometry.

providing pure production of vascular endothelial cells including VE-cadherin-negative "atypical" vascular endothelial cells.

The in vivo functions of ES-derived vascular endothelial cells

We next studied the in vivo functions of cmES-derived vascular endothelial cells by performing collagen sponge plug assays. Honeycomb collagen sponges were mixed with cmES-derived vascular endothelial cells (at passage 3) and transplanted intraperitoneally into SCID mice. After 35 days, FITC-dextran was injected from tail vein and then plugs were excited and histologically examined. As shown in Figure 8A, multiple FITC-dextran-filled lumens were detected in the collagen plugs, indicating the presence of neovascularization connected with systematic circulation within the plugs. Histological observations further confirmed the presence of neovascularization, which was filled with erythrocytes (Fig. 8B). The cells that lined the neovascular lumens as well as the cells remaining within the honeycomb plugs were all stained by both an anti-human HLA-A, B, C antibody (Fig. 8C, left middle part), which distinguishes primate cells from murine cells (Kaufman et al., 2004), and by an anti-human PECAM-1 antibody (Fig. 8C, right middle parts) which shows their endothelial nature. Finally, these vascular structures with human (primate)

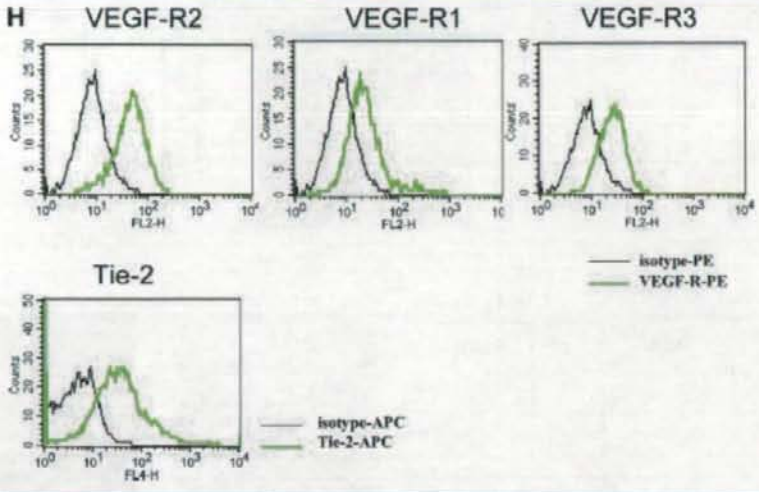

Fig. 5. ***(Continued)***

HLA and PECAM-1 were again shown to be connected with systematic circulation (Fig. 8C, lower left and right parts).

Thus, the cmES-derived vascular endothelial cells produced by our method are functional in vivo.

Evaluation of the roles of each medium component for effective differentiation

Finally, we re-evaluated the requirement of each component of our differentiation medium for vascular endothelial differentiation of cmES cells. First we studied the necessity of each cytokine for the generation of spheres, sac-like structures and cell surface VE-cadherin/PECAM-1-positive cells by checking the effects of depletion of each one cytokine from differentiation medium.

Depletion of IL-3 or IL-6 deteriorated the quality of spheres: the spheres often failed to proliferate during subsequent adherent culture (data not shown). In regard to the other four cytokines (BMP-4, SCF, Flt3-L, and VEGF), depletion of BMP-4 resulted in the formation of sac-like structures with poor hematopoiesis (Fig. 9A). On the other hand, depletion of SCF, Flt3-L and VEGF did not affect the formation of sac-like structures (Fig. 9A).

When estimated by the performance for the induction of cell surface VE-cadherin/PECAM-1-positive cells, all of the four cytokines BMP-4, SCF, Flt3-L and VEGF were found to play important roles in differentiation. Depletion of BMP-4, SCF, or Flt3-L deteriorated the performance levels in producing cell surface VE-cadherin/PECAM-1-positive cells (Fig. 9C,D). Although in some cases, depletion of each cytokine did not dramatically reduce the percentages of cell surface VE-cadherin/PECAM-1-positive cells (Fig. 9C), it did abolish the generation of cell surface VE-cadherin/PECAM-1-positive cells in other cases (Fig. 9B). Approximately estimated, one out of three experiments, we failed in generation of cell surface VE-cadherin/PECAM-1-double-positive cells when BMP-4, SCF, or Flt3-L was depleted from the medium. Depletion of VEGF reproducibly reduced the percentages of cell surface VE-cadherin/PECAM-1-positive cells (Fig. 9B,C). In contrast, replacement of IMDM by RPMI 1640 medium did not affect the all processes of differentiation (Fig. 9A–C). On the other hand, no sac-like structures were generated by EGM™-2 BulletKit cultures even when supplemented with six cytokines or six cytokines plus 10% FBS (Fig. 9A). In addition, percentages of cell surface VE-cadherin/PECAM-1-positive cells were considerably low (Fig. 9B–C), a finding almost identical to EGM™-2 BulletKit culture without six cytokines (Fig. 4A, EGM part).

Thus, it was concluded that (1) IL-3 and IL-6 contribute to the improvement of the quality of spheres, (2) BMP-4 is essential for a sac-dependent hematopoiesis, (3) VEGF is critical for the production of cell surface VE-cadherin/PECAM-1-positive cells, (4) BMP-4, SCF and Flt3-L contribute to the stable induction of cell surface VE-cadherin/PECAM-1-positive cells, and (5) Differentiation medium can be prepared by using RPMI 1640 in place of IMDM, but not by using EGM™-2 BulletKit, for the production of a sac-like structure and cell surface VE-cadherin/PECAM-1-positive cells.

Discussion

In this article, we reported a method for high efficiency differentiation of vascular endothelial cells from feeder-free primate ES cells. cmES-derived vascular endothelial cells are subculturable and freeze–thaw-tolerable. An additional merit of our system is its feasibility: it does not require a process to sort the progenitor populations such as VEGF-R2-positive (Sone et al., 2003, 2007) or CD34-positive (Wang et al., 2007) fractions. To our knowledge, this is the highest efficiency system for the production of vascular endothelial cells. Indeed, our system provides almost two pure populations: the cell surface VE-cadherin/PECAM-1-positive "canonical" vascular endothelial cells and cell surface VE-cadherin/PECAM-1-negative "atypical" vascular endothelial cells. Co-existence of pericytes was excluded. Contamination of immature Nanog-expressing ES cells was also excluded. Eventually, no tumor formation was observed after transplanting the cmES-derived vascular endothelial cells into SCID mice (data not shown), encouraging a safe application of

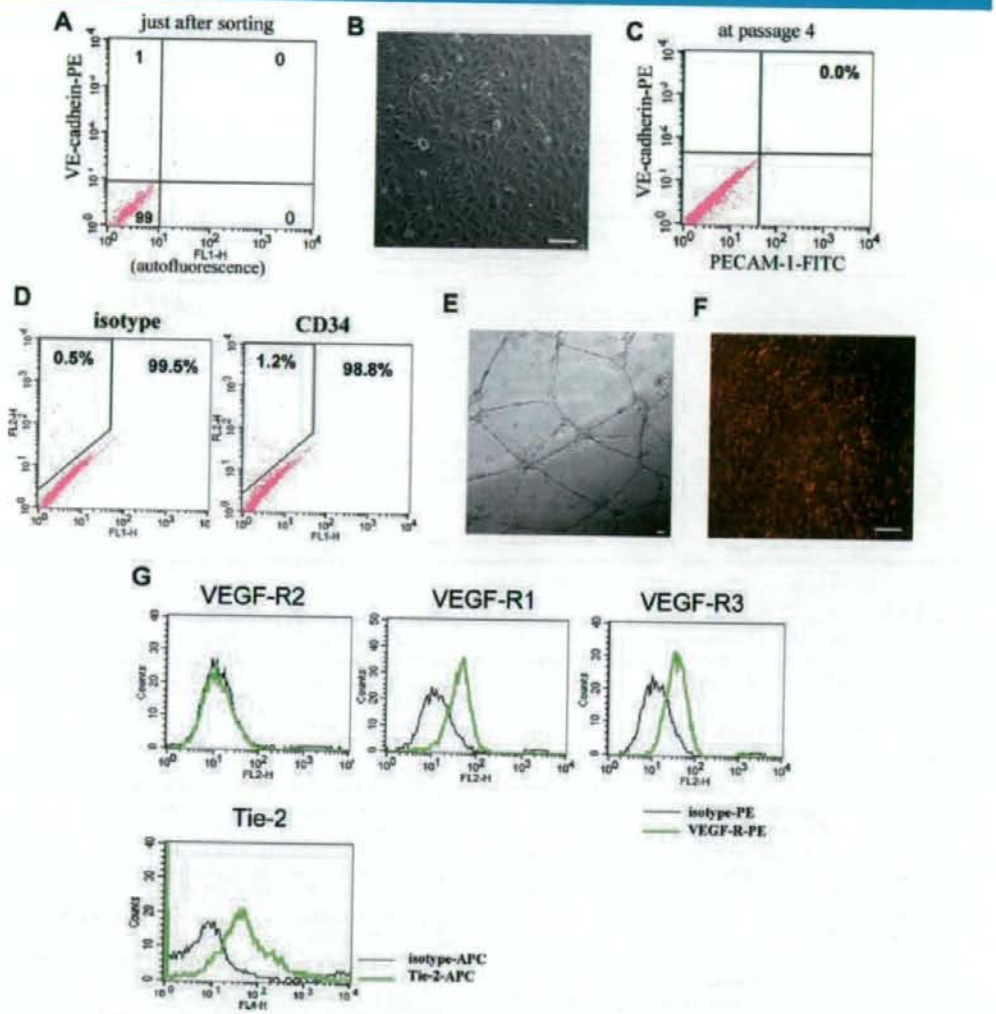

Fig. 6. Expansion and characterization of cell surface VE-cadherin-negative populations. Differentiation procedure was performed, and after the first passage, cell surface VE-cadherin-negative fraction was sorted by FACSAria™. A: The expression of VE-cadherin was determined just after sorting. B: After a few days culture, cell morphology was observed under an inverted phase contrast light microscope. The scale bar indicates 100 μm. C: After four passages, the cell surface expressions of VE-cadherin/PECAM-1 were re-studied by flow cytometry. D: The cell surface expression of CD34 was also studied by flow cytometry. E,F: The functional analyses. Cord-forming activities (E) and Ac-LDL-uptaking capacities (F) were confirmed. The scale bar indicates 100 μm. G: Cell surface expressions of other endothelial markers (VEGF-R2, VEGF-R1, VEGF-R3, and Tie-2) were studied by flow cytometry. H: VE-cadherin expression was determined by immunostaining studies. The cells were stained by an anti-VE-cadherin antibody (upper) or isotype control antibody (lower). The right parts indicate the phase contrast microscopy. The scale bar indicates 50 μm. I: Western blotting of VE-cadherin (left) and β-tubulin (right) of the cell surface VE-cadherin-negative population (lane 1) and the total population before sorting (lane 2). The expression of 130-kDa VE-cadherin band (indicated by arrow) was detected even in the cell surface VE-cadherin-negative population, indicating the intracellular localization of VE-cadherin. J: RT-PCR studies for VE-cadherin (upper) and β-actin (lower) were shown. The templates used were as follows: lane 1; cDNA of the cell surface VE-cadherin-negative population, lane 2; cDNA of total populations before sorting, lane 3; cDNA of HUVEC, lane 4; water, lane 5; cDNA of hematopoietic HL-60 cells. K,L: Immunostaining studies and flow cytometric analyses of hematopoietic and monocyte/macrophage markers. K: Cells were stained by an isotype control antibody (left) or an anti-CD68 antibody (right). Lower parts indicate the photographs with Normarsky differentiated interference contrast. The scale bar indicates 100 μm. L: Cell surface expressions of CD14 (upper, a bold green line), CD18 (middle, a bold green line), CD11b (lower, a bold green line), and CD45 (lower, a bold pink line) were studied. Thin black lines indicate the data of non-staining samples and bold black lines indicate the data of isotype control antibody-stained samples.

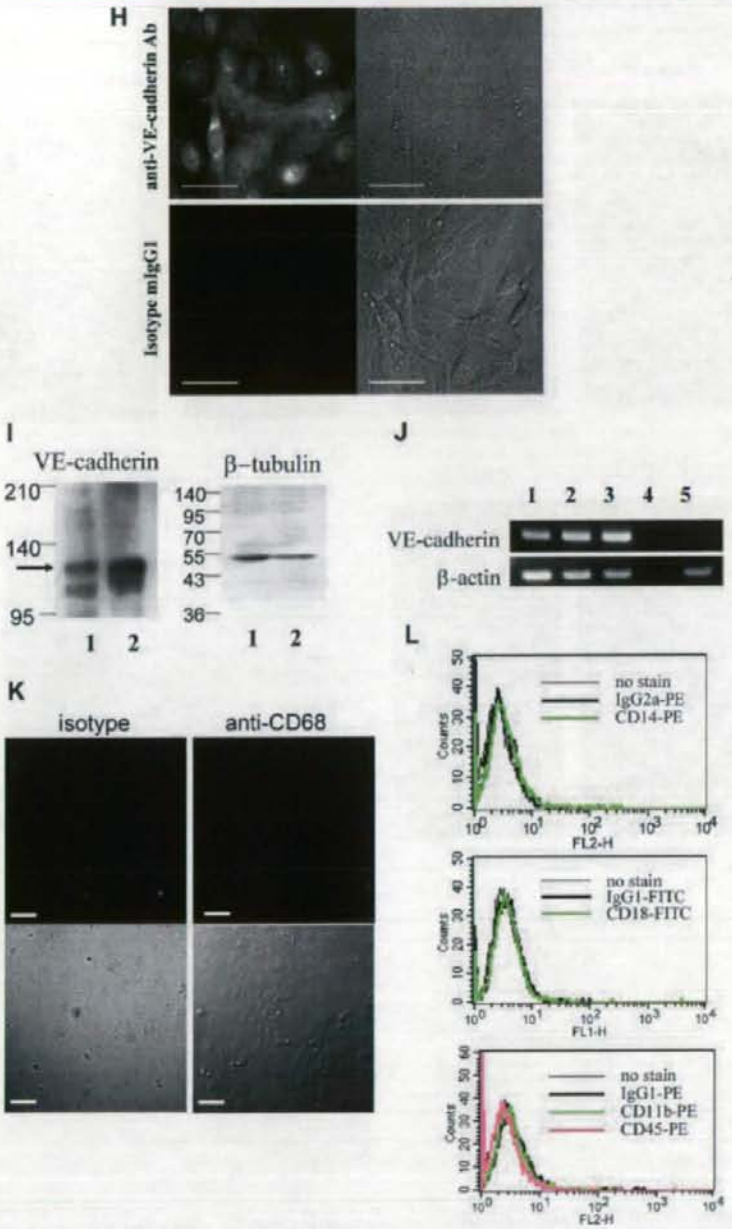

Fig. 6. ***(Continued)***

human ES-derived endothelial cells to clinical purposes in future.

Technically, our differentiation method has two unique points. One is the two-step protocol, where a sphere formation is followed by adherent culture. Although a short sphere-forming process was performed in our system, we could obtain clear microscopic fields owing to the subsequent adherent culture step, during which cells proliferated and

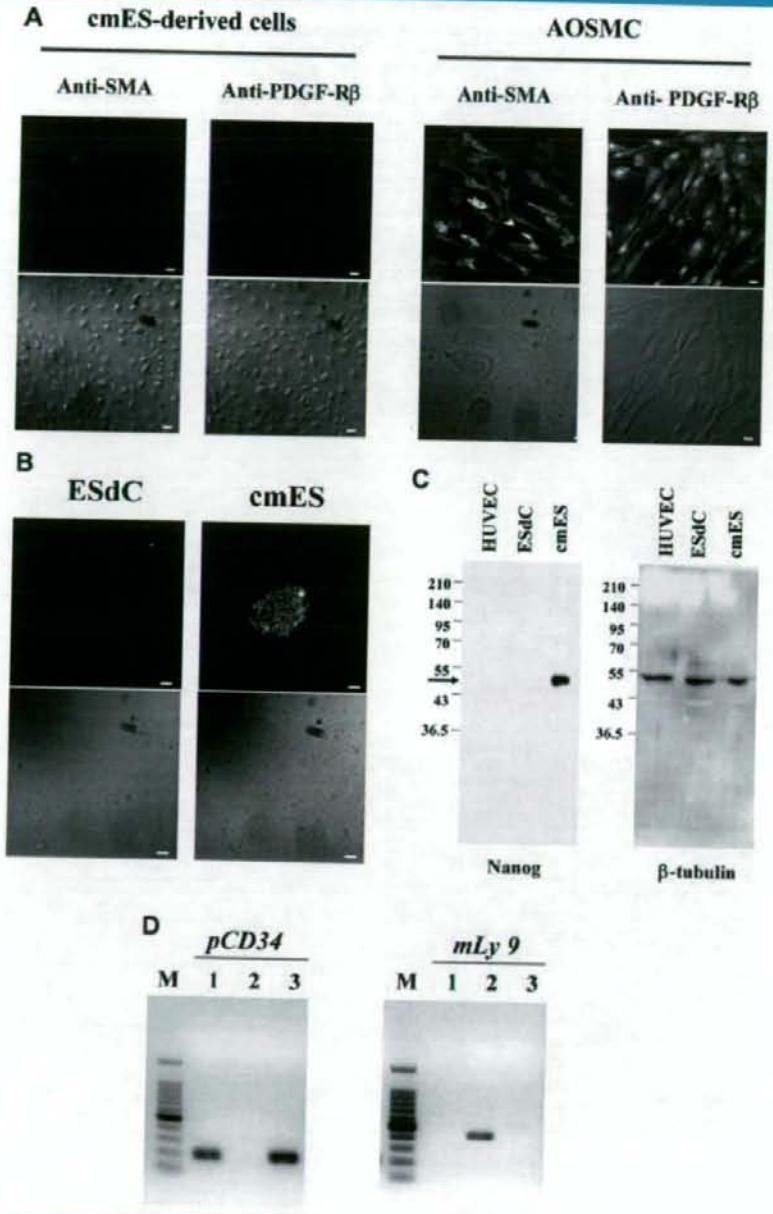

Fig. 7. Possible existence or contamination of pericytes, undifferentiated ES cells and MEFs was investigated. A: Possible existence of pericytes in cmES-derived cells was studied based upon smooth muscle specific markers (SMA and PDGF-Rβ). cmES-derived cells (left parts) were fixed and stained by anti-SMA antibody or anti-PDGF-Rβ antibody as indicated. As a positive control, human aortic smooth muscle cells (AOSMC) were used. The scale bar indicates 20 μm. B,C: Possible existence or contamination of undifferentiated cmES cells in cmES-derived cells (ESdC) was studied based upon undifferentiated ES cell marker, Nanog. The ESdC or undifferentiated cmES cells were fixed and stained by anti-human Nanog antibody (B) or were lysed and subjected to Western blotting using anti-Nanog antibody (C, left). An arrow indicates the expression of 50-kDa Nanog protein. For internal control, β-tubulin expression was examined (C, right). The scale bar indicates 100 μm. D: Possible contamination of MEFs in cmES-derived cells was studied using primate and murine specific markers. Genomic DNA was extracted from HUVECs (lane 1), MEFs (lane 2), and cmES-derived cells (lane 3). PCR was performed using the primers for primate CD34 genomic fragment (left column; *pCD34*) or those for murine ly 9.2 genomic fragment (right column; *mLy9*).

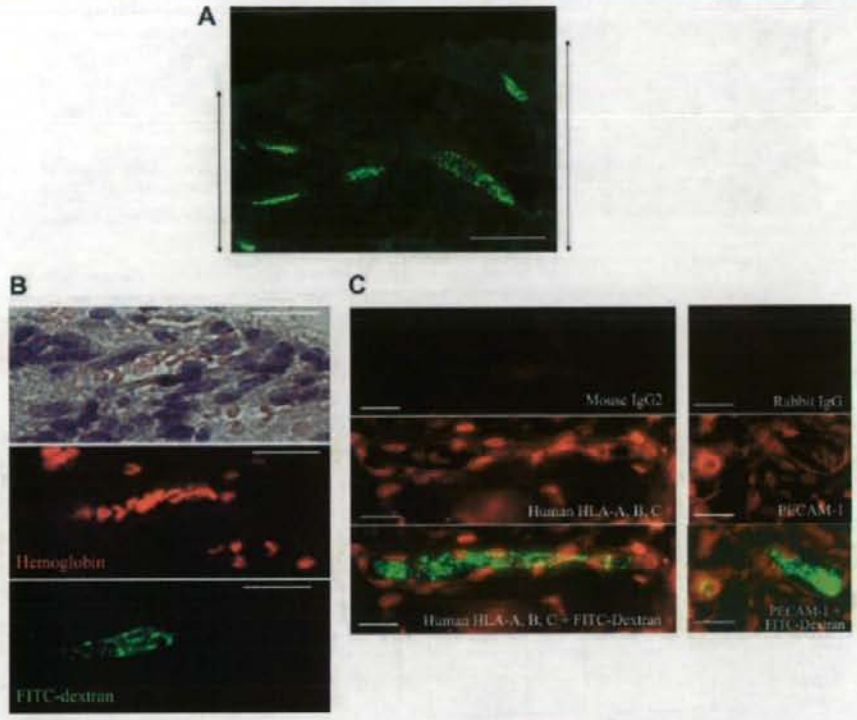

Fig. 8. The in vivo functions of cmES-derived cells. cmES-derived cells were cultured in honeycomb collagen sponges for 2 days in vitro and were then transplanted intraperitoneally into SCID mice. At day 35, FITC-dextran was injected into the transplanted mouse from a tail vein. Then collagen plugs were taken out, fixed, embedded and sliced as described in Materials and Methods Section. A: Fluorescence microscopic observations of FITC-dextran in sliced honeycomb collagen sponges. The scale bar indicates 100 μm. B: The microscopic observation of hematoxylin-eosin-stained samples (upper) and fluorescence microscopic observations of autofluorescence of hemoglobins (middle) and FITC-dextran (lower). Scale bars indicate 20 μm. C: Immunostaining studies were performed using indicated antibodies. The positive staining by anti-human PECAM-1 and anti-human HLA-A, B, C antibodies indicates the recruitment of cmES-derived cells into the neovascularity. Scale bars indicate 20 μm.

spread out almost like a monolayer culture. Hence, we could identify a unique construction, a sac-like structure surrounded by cobblestone cells, as the parental organization for vascular endothelial cells. Recently, the existence of this "sac-like" structure was independently reported (Ma et al., 2007), where human ES cells were co-cultured with murine OP9 stromal cells. Interestingly, they reported that the sac-like structures emerged with the same time course (around 12 days after co-culture) as our system. Because we applied the feeder-free culture method, we could detect the presence of surrounding cobblestone cells, which might possibly be merged with OP9 cells in their system. By immunostaining studies, we further noticed that both sac wall cells and surrounding cobblestone cells expressed VE-cadherin at intercellular junctions (Fig. 1D).

Another point of our success may reside in the formula of our differentiation medium. In contrast to previous reports, where a commercially available vascular endothelial cell-specific medium of EGM®-2 MV BulletKit was used (Kaufman et al., 2004; Wang et al., 2007), we prepared the differentiation medium by modifying the culture medium optimized to hematopoietic differentiation (Li et al., 2001). As our original aim was to produce hematopoietic stem cells, we deleted GM-CSF, G-CSF, erythropoietin and hydrocortisone, which rather work in later and mature phases of hematopoiesis, from the formula by Li et al. (2001). After we had established our method for high efficiency differentiation of vascular endothelial cells, we re-evaluated the necessity of each cytokine and found that the differentiation medium was indeed optimal. Among six cytokines, the role of VEGF is very clear: it is required for production of cell surface VE-cadherin/PECAM-1-positive population. Other cytokines including BMP-4, IL-3, IL-6, SCF and FLt3-L are required for the better performance of differentiation. Literally, BMP-4 is required for the generation of Scl/Tal-1-positive hemangioblast cells from murine ES cells (Park et al., 2004). IL-3 and SCF are reportedly effective in inducing vascular endothelial cells from murine hematopoietic cells (Yamada and Takakura, 2006). Recently, it was reported that IL-6 promotes choroidal neovascularization (Izumi-Nagai et al., 2007). Thus, it seems that every hematopoietic cytokine is involved in specific phase of vascular endothelial differentiation although its precise roles are not yet determined. Our usage of multiple hematopoietic cytokines possibly contributed to the prevention of emergence and/or proliferation of pericytes, which are often generated with vascular endothelial cells during

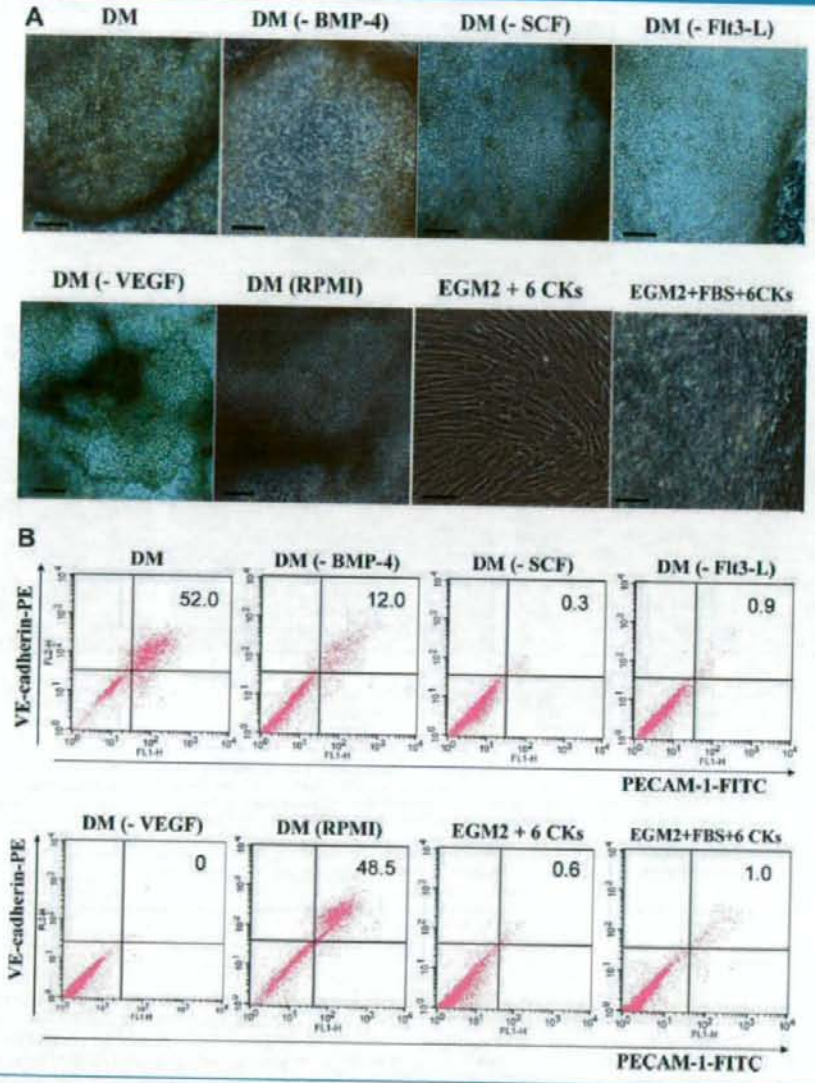

Fig. 9. The roles of medium components for vascular endothelial differentiation. The differentiation procedure was performed by depleting BMP-4 (DM(-BMP-4)), SCF (DM(-SCF)), Flt3-L (DM(-Flt3-L)) or VEGF (DM(-VEGF)) from the differentiation medium (DM), using differentiation medium prepared by using RPMI 1640 in place of IMDM (DM(RPMI)), using EGM™-2 BulletKit medium supplemented with all six cytokines (EGM2 + 6CKs), or using EGM™-2 BulletKit medium supplemented with 10% FBS and all six cytokines (EGM2 + FBS + 6CKs). A: The phase contrast micrographs. Note that BMP-4 depletion resulted in deficient production of inner round cells. Scale bars indicate 50 μm. B,C: Flow cytometric analyses for cell surface VE-cadherin/PECAM-1 expressions. From a number of experiments, we obtained two patterns of results shown in (B) and (C) with 1:2 frequencies (data not shown).

differentiation of ES cells and inhibit the expansion of vascular endothelial cells. Of course, further studies are required for the total understanding of the hematopoietic/endothelial differentiation mechanism from primate ES cells.

In this report, we termed the cells that are cell surface VE-cadherin/PECAM-1-negative but otherwise are equivalent to vascular endothelial cells as "atypical vascular endothelial cells." These cells seem to be frequently produced during primate ES differentiation (Kaufman et al., 2004). Whether the existence of atypical vascular endothelial cells is restricted to in vitro differentiation system or there are in vivo counterparts is a matter of great interest. It is known that fractions of adult human peripheral monocytes can give rise to endothelial-like cells. For example, monocyte-derived immature dendritic cells

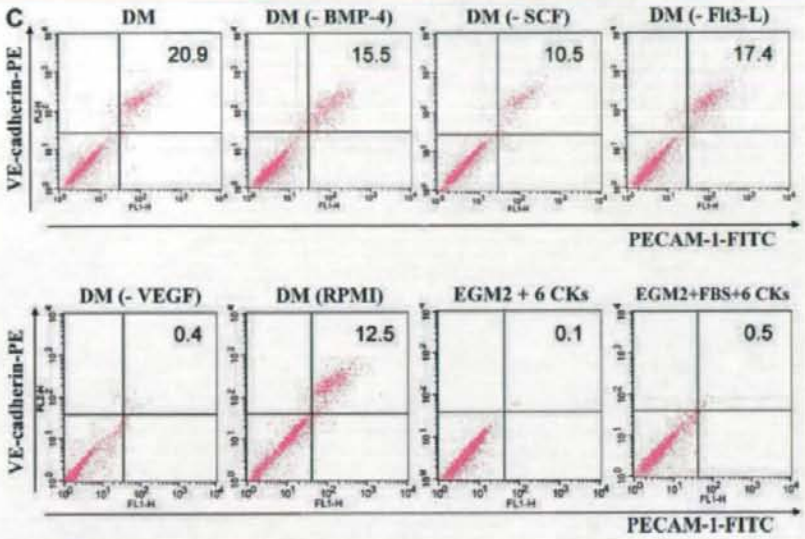

Fig. 9. ***(Continued)***

(Fernandez Pujol et al., 2001) and monocyte-derived multi-potential cells (Kuwana et al., 2006) can produce functionally maturated vascular endothelial cells. Our cmES-derived cells are, however, negative for monocyte markers including CD68, CD14 and CD11b (Fig. 6K,L). As for now, it is not yet determined whether they belong to a novel endothelial population or they represent a transient state during which monocytic precursors are differentiating into vascular endothelial cells. Future investigation will be required for the evaluation of atypical vascular endothelial cells in vivo.

The ES-derived vascular endothelial cells generated by our method are subculturable up to eight passages, after which they undergo senescence (unpublished observation). Aging cells show enlarged morphologies and become positive in senescence-associated β-galactosidase activity assays along with p38 activation and p16 induction. The reason for this stress-induced senescence remains elusive. Although the senescence induction in ES-derived vascular endothelial cells may put certain restrictions on their usage, it may exclude the possible tumorigenesis via unlimited proliferation after transplantation. Moreover, our ES-derived vascular endothelial cells can be used for researches on stress-induced senescence, providing tools for investigations on mechanisms of vascular complication development in lifestyle-related stress-associated diseases such as diabetes mellitus (Yokoi et al., 2006) hypertension (Kobayashi et al., 2006) and atherosclerosis (Minamino et al., 2002).

Our differentiation method is applicable to human ES cells: the high efficiency vascular endothelial differentiation (~70%) with proper in vitro and in vivo functions has been achieved by using human ES cells and the same differentiation protocol (M. Nakahara, in preparation). Of course, human ES cells cannot be directly applied to regenerative medicine because of an immunological hurdle. However, when the hurdle will be overcome via a nuclear transfer technique (Byrne et al., 2007) or when iPS cells (Takahashi et al., 2007; Yu et al., 2007) will be improved for safety application to clinical usages, our method will provide the most effective tool for regenerative medicine targeted to vascular endothelial disorders.

Literature Cited

Byrne JA, Pedersen DA, Clepper LL, Nelson M, Sanger WG, Gokhale S, Wolf DP, Mitalipov SM. 2007. Producing primate embryonic stem cells by somatic cell nuclear transfer. Nature 450:497–502.

Fernandez Pujol B, Lucibello FC, Zuzarte M, Lütjens P, Müller R, Havemann K. 2001. Dendritic cells derived from peripheral monocytes express endothelial markers and in the presence of angiogenic growth factors differentiate into endothelial-like cells. Eur J Cell Biol 80:99–110.

Hirashima M, Kataoka H, Nishikawa S, Matsuyoshi N, Nishikawa S. 1999. Maturation of embryonic stem cells into endothelial cells in an in vitro model of vasculogenesis. Blood 93:1253–1263.

Izumi-Nagai K, Nagai N, Ozawa Y, Mihara M, Ohsugi Y, Kurihara T, Koto T, Satofuka S, Inoue M, Tsubota K, Okano H, Oike Y, Ishida S. 2007. Interleukin-6 receptor-mediated activation of signal transducer and activator of transcription-3 (STAT3) promotes choroidal neovascularization. Am J Pathol 170:2149–2158.

Kaufman DS, Lewis RL, Hanson ET, Auerbach R, Plendl J, Thomson JA. 2004. Functional endothelial cells derived from rhesus monkey embryonic stem cells. Blood 103:1325–1332.

Kobayashi K, Imanishi T, Akasaka T. 2006. Endothelial progenitor cell differentiation and senescence in an angiotensin II-infusion rat model. Hypertens Res 29:449–455.

Kuwana M, Okazaki Y, Kodama H, Satoh T, Kawakami Y, Ikeda Y. 2006. Endothelial differentiation potential of human monocyte-derived multipotential cells. Stem Cells 24:2733–2743.

Levenberg S, Golub JS, Amit M, Itskovitz-Eldor J, Langer R. 2002. Endothelial cells derived from human embryonic stem cells. Proc Natl Acad Sci USA 99:4391–4396.

Li F, Lu S, Vida L, Thomson JA, Honig GR. 2001. Bone morphogenetic protein 4 induces efficient hematopoietic differentiation of rhesus monkey embryonic stem cells in vitro. Blood 15:335–432.

Ma F, Wang D, Hanada S, Ebihara Y, Kawasaki H, Zaike Y, Heike T, Nakahata T, Tsuji K. 2007. Novel method for efficient production of multipotential hematopoietic progenitors from human embryonic stem cells. Int J Hematol 85:371–379.

Minamino T, Miyauchi H, Yoshida T, Ishida Y, Yoshida H, Komuro I. 2002. Endothelial cell senescence in human atherosclerosis: Role of telomere in endothelial dysfunction. Circulation 105:1541–1544.

Park C, Afrikanova I, Chung YS, Zhang WJ, Arentson E, Fong Gh G, Rosendahl A, Choi K. 2004. A hierarchical order of factors in the generation of FLK1- and SCL-expressing hematopoietic and endothelial progenitors from embryonic stem cells. Development 131:2749–2762.

Saeki K, Hong Z, Nakatsu M, Yoshimori T, Kabeya Y, Yamamoto A, Kaburagi Y, Yuo A. 2003. Insulin-dependent signaling regulates azurophil granule-selective macroautophagy in human myeloblastic cells. J Leukoc Biol 74:1108–1116.

Sato N, Meijer L, Skaltsounis L, Greengard P, Brivanlou AH. 2004. Maintenance of pluripotency in human and mouse embryonic stem cells through activation of Wnt signaling by a pharmacological GSK-3-specific inhibitor. Nat Med 10:55–63.

Sone M, Itoh H, Yamashita J, Yurugi-Kobayashi T, Suzuki Y, Kondo Y, Nonoguchi A, Sawada N, Yamahara K, Miyashita K, Park K, Shibuya M, Nito S, Nishikawa S, Nakao K. 2003.

Different differentiation kinetics of vascular progenitor cells in primate and mouse embryonic stem cells. Circulation 107:2085–2088.

Sone M, Itoh H, Yamahara K, Yamashita JK, Yurugi-Kobayashi T, Nonoguchi A, Suzuki Y, Chao TH, Sawada N, Fukunaga Y, Miyashita K, Park K, Oyamada N, Sawada N, Taura D, Tamura N, Kondo Y, Nito S, Suemori H, Nakatsuji N, Nishikawa S, Nakao K. 2007. Pathway for differentiation of human embryonic stem cells to vascular cell components and their potential for vascular regeneration. Arterioscler Thromb Vasc Biol 27:2127–2134.

Suemori H, Tada T, Torii R, Hosoi Y, Kobayashi K, Imahie H, Kondo Y, Iritani A, Nakatsuji N. 2001. Establishment of embryonic stem cell lines from cynomolgus monkey blastocysts produced by IVF or ICSI. Dev Dyn 222:273–279.

Takagi Y, Takahashi J, Saiki H, Morizane A, Hayashi T, Kishi Y, Fukuda H, Okamoto Y, Koyanagi M, Ideguchi M, Hayashi H, Imazato T, Kawasaki H, Suemori H, Omachi S, Iida H, Itoh N, Nakatsuji N, Sasai Y, Hashimoto N. 2005. Dopaminergic neurons generated from monkey embryonic stem cells function in a Parkinson primate model. J Clin Invest 115: 102–109.

Takahashi K, Tanabe K, Ohnuki M, Narita M, Ichisaka T, Tomoda K, Yamanaka S. 2007. Induction of pluripotent stem cells from adult human fibroblasts by defined factors. Cell 131:861–872.

Vodyanik MA, Bork JA, Thomson JA, Slukvin II. 2005. Human embryonic stem cell-derived CD34+ cells: Efficient production in the coculture with OP9 stromal cells and analysis of lymphohematopoietic potential. Blood 105:617–626.

Wang ZZ, Au P, Chen T, Shao Y, Daheron LM, Bai H, Arzigian M, Fukumura D, Jain RK, Scadden DT. 2007. Endothelial cells derived from human embryonic stem cells form durable blood vessels in vivo. Nat Biotechnol 25:317–318.

Yamada Y, Takakura N. 2006. Physiological pathway of differentiation of hematopoietic stem cell population into mural cells. J Exp Med 203:1055–1065.

Yamashita J, Itoh H, Hirashima M, Ogawa M, Nishikawa S, Yurugi T, Naito M, Nakao K, Nishikawa S. 2000. Flk1-positive cells derived from embryonic stem cells serve as vascular progenitors. Nature 408:92–96.

Yokoi T, Fukuo K, Yasuda O, Hotta M, Miyazaki J, Takemura Y, Kawamoto H, Ichijo H, Ogihara T. 2006. Apoptosis signal-regulating kinase 1 mediates cellular senescence induced by high glucose in endothelial cells. Diabetes 55:1660–1665.

Yu J, Vodyanik MA, Smuga-Otto K, Antosiewicz-Bourget J, Frane JL, Tian S, Nie J, Jonsdottir GA, Ruotti V, Stewart R, Slukvin II, Thomson JA. 2007. Induced pluripotent stem cell lines derived from human somatic cells. Science 318:1917–1920.

CLONING AND STEM CELLS
Volume 10, Number 2, 2008

DOI: 10.1089/clo.2007.0068

A Feeder-Free Hematopoietic Differentiation System with Generation of Functional Neutrophils from Feeder- and Cytokine-Free Primate Embryonic Stem Cells

MASAKO NAKAHARA,[1] SATOKO MATSUYAMA,[1] KUMIKO SAEKI,[1] NAOKO NAKAMURA,[1] KOICHI SAEKI,[1] YOSHIKO YOGIASHI,[1] ASAKO YONEDA,[1] MAKOTO KOYANAGI,[1] YASUSHI KONDO,[2] and AKIRA YUO[1]

ABSTRACT

We have established a novel feeder- and recombinant cytokine-free culture system for the maintenance of primate embryonic stem (ES) cells along with a feeder-free hematopoietic differentiation protocol for high efficiency CD45-positive cell production. In our system, cynomolgus monkey ES cells were properly maintained in an undifferentiated state with high immature marker expressions and teratoma-producing activities. Embryoid bodies (EBs) were generated in the presence of serum and cytokine cocktail and subjected to attachment culture on gelatin-coated plates. After about 2 weeks, a sac-like structure filled with abundant round cells emerged at the center of flattened EB. Then total cells were collected and transferred onto new gelatin-coated plates, where cells were firmly attached and actively proliferated to confluence. After another few days culture, abundant floating cells were detected in the culture supernatant. These cells expressed high levels of CD45 (>90%), while adherent cells expressed low levels of CD45 (<10%). The former consisted of various differentiated stages of myeloid cells from immature myeloblasts to mature polymorphonuclear neutrophils and macrophages. Although the percentages of neutrophils varied between 10 to 20 depending on experiments, their mature phenotype was reproducibly confirmed by specific staining and functional assays. Although dispensable for the generation of hematopoietic cells, serum is essential for the production of mature neutrophils and macrophages. Our protocol provides the minimum essence for primate ES cell maintenance and hematopoietic differentiation that is beneficial from economical and clinical points of view.

INTRODUCTION

EMBRYONIC STEM (ES) CELLS are a valuable resource in regenerative medicine because of their high capacity to differentiate into a broad range of cell types. Although the study on human ES cells is essential for clinical applications, basic researches using monkey ES cells still has great importance because these cells provide good transplantation models that must be used in the preclinical studies (Takagi et al., 2005). Moreover, the use of monkey ES cells avoids ethical issues and thus biotechnological manipulation of them, including gene transfer, can immediately be ap-

[1]Department of Hematology, Research Institute, International Medical Center of Japan, Tokyo, Japan.
[2]Regenerative Medicine Group, Advanced Medical Research Laboratory, Mitsubishi Tanabe Pharma Corporation, Osaka, Japan.

plied, which will contribute to advancing our understanding of human ES cells.

By contrast to murine ES cells, neither leukemia-inhibitory factor nor bone morphogenetic proteins is effective to maintain primate ES cells in undifferentiated states. In the first successful report concerning the feeder-free maintenance of primate ES cells, conditioned medium (CM) of mouse embryonic fibroblasts (MEF), namely MEF-CM, was used (Xu et al., 2001). Afterward, several MEF-CM-free methods have been reported to meet a clinical requirement, avoiding coexistence of mouse cell-derived factors (Amit et al., 2004; Beattie et al., 2005; Chen et al., 2006; Ludwig et al., 2006; Sato et al., 2004; Wang et al., 2005; C. Xu et al., 2005; R.H. Xu et al., 2005; Yao et al., 2006). Although certain small-molecular-weight chemical substances are reportedly effective in the maintenance of primate ES cells (Chen et al., 2006; Sato et al., 2004), their safety has not been verified yet. All the other methods exclusively adopt high-dose usage of cytokines and growth factors including fibroblast growth factor (FGF)-2, Noggin, transforming growth factor (TGF)-β and Activin, which may rather be a disadvantage from economical standpoints. Moreover, involvement of these cytokines in the self-renewal of inner cell mass, an *in vivo* counterpart of primate ES cells, remains undetermined. Thus, it has been an open question whether the usage of these cytokines is really essential for the maintenance of primate ES cells or sophistication in culture technique can spare the requirement of these cytokines. It is widely accepted that the cell density is an important factor for the maintenance of primate ES cells (Xu et al., 2001). In addition, the size of ES colonies would also be a determinant factor, because FGF-2 reportedly prevents differentiation of ES cells located at marginal regions of the colony, whereas Noggin prevents differentiation of the cells located at center regions (R.H. Xu et al., 2005). It has also been suggested that murine (Niwa et al., 2004) and primate (Hishikawa, 2006) ES cells produce autocrine factors to keep themselves in an immature states. All these findings together suggest that ES cells can be maintained in an undifferentiated state by autocrine factors via an appropriate control of the size and density of ES colonies in the absence of exogenous cytokines.

As for hematopoietic differentiation of ES cells, there are two major approaches. One is coculturing ES cells with stromal cells such as murine OP9, MS-5 and/or C3H10T1/2 cells as the feeders (Hiroyama et al., 2006; Nakano et al., 1996; Umeda et al., 2004; Vodyanik et al., 2005). Although feeder cells have large capacities to promote the directed differentiation and to maintain the viability of differentiated cells, contamination of the final products by feeder cells or antigens transmitted by the feeder cells (Martin et al., 2005) cannot completely be excluded even if cell-sorting processes are appropriately performed. For the production of materials suitable for clinical applications, the second approach, the feeder-free culture system with embryoid body (EB) formation, would be desirable. EB formation is principally a random differentiation process, and thus, directed differentiation into a specific tissue seems impossible. However, concerning hematopoietic differentiation, a highly efficient production of CD45-positive hematopoietic cells has been reported by the culture methods to use high-dose hematopoietic growth factors (Chadwick et al., 2003; Wang et al., 2004).

Here we report a novel feeder- and cytokine-free culture system for maintenance of primate ES cells and a unique feeder-free hematopoietic differentiation protocol that enables production of functional neutrophils. In the former, we show that careful cell manipulation to keep the size and number of ES colonies within an appropriate range during routine subculture has simply enabled the maintenance of primate ES cells without cytokines and growth factors added exogenously. In the latter, we generated EBs by floating culture in the first step of the culture and subsequently subjected them to attachment culture as a second step. This sequential combination culture technique has been reported in the differentiation of nonhematopoietic cells including retinal cells (Ikeda et al., 2005), neuronal cells (Calhoun et al., 2003), hepatocyte (Yin et al., 2007), and chondrocytes (Hwang et al., 2006). However, no trials have been reported concerning hematopoietic differentiation. By virtue of attachment monolayer culture in later step, we could get clear microscopic observation fields, and thus, identified for the first time a unique construction, a sac-like structure filled with abundant round cells, as a precursory organization of ES-derived hematopoiesis *in vitro*. Moreover, we could obtain CD45-positive hematopoietic cell-rich (>90%) populations without using cell-sorting apparatus by simple collection of floating cells from culture medium.

Our culture system provides the most simplified and feasible method for the maintenance and high efficiency production of hematopoietic cells from primate ES cells. Our method is highly beneficial in performing ES cell studies under natural conditions, free from possible disturbing effects of exogenously added cytokines, and also in preparing large-scaled materials for clinical purposes in an economically sensible way.

MATERIALS AND METHODS

Culture of undifferentiated cynomolgus monkey ES cells

Murine embryonic fibroblasts (MEFs), which had been treated with Dulbecco modified Eagle medium (DMEM) containing mitomycin C (MMC) (Sigma Chemical Co., St. Louis, MO) for 3 h, were seeded on the dishes coated with 0.1% gelatin. Cynomolgus monkey ES cells (CMK-6) (Suemori et al., 2001) were maintained on MMC-treated MEF-coated dishes in DMEM/F12 medium (Invitrogen Corp., Carslbad, CA) supplemented with 20% Knockout™ Serum Replacement (Invitrogen Corp.), 1% nonessential amino acids solution (Invitrogen Corp.), 1 mM Sodium Pyruvate Solution (Invitrogen Corp.), 2 mM L-glutamine (Invitrogen Corp.), 10 U/mL penicillin (Invitrogen Corp.), and 10 μg/mL streptomycin (Invitrogen Corp.) under a standard gas atmosphere humidified air/5% CO_2. ES cells were passed twice a week by collagenase treatment and seeded at split ratios of 1:2 to 1:4 on new MEF-coated dishes. For the feeder-free and cytokine-free culture, cynomolgus monkey ES cells were maintained on Matrigel™ Matrix (Invitrogen Corp.) coated on 78 cm^2 culture flasks in DMEM/F12 medium (Invitrogen Corp.) supplemented with 20% Knockout™ Serum Replacement (Invitrogen Corp.), 1% nonessential amino acids solution (Invitrogen Corp.), 1 mM sodium pyruvate solution (Invitrogen Corp.), 2 mM L-glutamine (Invitrogen Corp.), 10 U/mL penicillin (Invitrogen Corp.), and 10 μg/mL streptomycin (Invitrogen Corp.) under a standard gas atmosphere humidified air/5% CO_2. The ES cells were maintained as colonies with similar sizes, and the diameters of colonies were about 400 μm after cell passage and about 800 μm just before subculture. The density of ES colonies was kept within an appropriate range, that is, from 4 to 5 colonies per 10 cm^2. The ES cells were passed three times a week. For detachment of the cells from the flasks, culture supernatant was aspirated and 1 mL of dispase (BD Biosciences, San Jose, CA) was added. Immediately, dispase solution was aspirated and the cells were incubated at 37°C for 10 min. Then Hanks' balanced salt solution (HBSS) was gently added to inactivate dispase after mild mixing. Cell suspension in HBSS was then transferred into a conical tube and the cells were collected by mild centrifugation. During all these procedures, pipetting of cell suspensions was not performed. Cells were seeded at split ratios of 1:2 on fresh Matrigel™ Matrix-coated flasks with careful and gentle shaking for homogenous distribution. Culture medium was changed every day. The ES cells maintained by this novel method were freeze–thaw-tolerable by a method as described elsewhere (Fujioka et al., 2004) and were able to be kept in liquid nitrogen at least for 1 month.

Teratoma formation

Cynomolgus monkey ES cells (1×10^5) maintained by our novel feeder-free method were injected beneath the capsule of the testis of adult male severe combined immunodeficient (SCID) mice (Stojkovic et al., 2005). After 8 weeks, mice were sacrificed and testes were removed. After tumor formation was checked by megascope, tumor tissues were fixed, sliced, and stained by hematoxylin and eosin solutions for subsequent histological examinations.

Embryoid body (EB) formation

EBs were formed according to the methods reported by Chadwick et al. (2003) with a minor modification. On the day of passage, undifferentiated ES cell colonies on a 78 cm^2 culture flask were collected by collagenase IV treatment at room temperature for 20 min followed by a treatment with nonenzymatic cell dissociation buffer (Invitrogen Corp.) at room temperature for 20 min. By these treatments, ES cell colonies were dissociated in single cells. The 1×10^6 ES cells were transferred to a 6-cm diameter low-attachment dish, which had been treated with 0.02% poly(2-hydroxyethyl methacrylate) (Sigma Chemical Co) dissolved in acetone/methanol (1:1) solution in a short while, to allow for EB formation by overnight incubation in 4 mL of differentiation medium consisting of Knockout D-

MEM (Invitrogen Corp.) supplemented with 20% heat-inactivated fetal bovine serum (FBS) (PAA Laboratories GmbH, Linz, Austria), 1% nonessential amino acids (Invitrogen Corp.), 0.1 mM β-mercaptoethanol (Sigma Chemical Co.), 1 mM L-glutamine (Invitrogen Corp.), 10 U/mL penicillin (Invitrogen Corp.), and 10 μg/mL streptomycin (Invitrogen Corp.). The next day cultures were given fresh differentiation medium consisting of Knockout D-MEM (Invitrogen Corp.) supplemented with 20% heat-inactivated FBS (PAA Laboratories GmbH), 1% nonessential amino acids (Invitrogen Corp.), 0.1 mM β-mercaptoethanol (Sigma Chemical Co.), 1 mM L-glutamine (Invitrogen Corp.), 10 U/mL penicillin (Invitrogen Corp.), 10 μg/mL streptomycin (Invitrogen Corp.), 50 ng/mL bone morphogenic protein 4 (BMP-4; R&D Systems Inc., Minneapolis, MN), 300 ng/mL stem cell factor (SCF; Pepro Tech Inc., Rocky Hill, NJ), 300 ng/mL Flt3 ligand (Flt3-L; Pepro Tech Inc.), 10 ng/mL interleukin 3 (IL-3; Pepro Tech Inc.), 10 ng/mL interleukin 6 (IL-6; Pepro Tech Inc.), and 50 ng/mL granulocyte colony-stimulating factor (G-CSF; Kirin Brewery Company, Ltd., Tokyo, Japan). EBs were cultured for 15 days with media and treatment changes every 3 days.

Subculture of EBs for an expanded reproduction of hematopoietic cells

EBs cultured for 15 days in a 6-cm diameter low-attachment dishes were then transferred onto a 0.1% gelatin B (Sigma Chemical Co.)-treated 10-cm diameter dish using the differentiation medium supplemented with cytokine cocktail above described. Medium was changed twice a week. After about a 2-week culture, sac-like structures that were filled with abundant round cells emerged. Then the total cells in the dishes were collected by trypsin/EDTA (Sigma Chemical Co.) treatment, transferred onto new gelatin-coated dishes, and subcultured using cytokine-supplemented differentiation media on the new gelatin-coated dishes. Within a few days, abundant floating cells were observed in the culture supernatant. The attached cells were passed on a fresh gelatin-coated dish twice a week with 1:2–1:4 dilution. The floating cells were collected *ad libitum* and used for assays.

Wright-Giemsa staining and special staining procedures

The viable cells in the dishes were directly observed under an inverted phase contrast light microscope (Olympus Optical Co. Ltd., Tokyo, Japan), or alternatively, the cells were fixed on slide glasses using a cytospin apparatus (Cytospin 2, SHANDON, Pittsburgh, PA), stained with Wright-Giemsa (WG) solution (Muto Pure Chemical Co., Tokyo, Japan), and then observed under the light microscope (Olympus Optical Co. Ltd.). Myeloperoxidase (MPO) staining, esterase double staining (α-naphthyl butyrate esterase and naphthol-ASD-chloroacetate esterase), and neutrophil alkaline phosphatase (NAP) staining were performed using corresponding staining kits (Muto Pure Chemical Co.) according the manufacturer protocols.

Determination of cell surface molecules by flow cytometric analysis

Cell surface markers of cynomolgus ES cells and ES-derived differentiated cells were analyzed by flow cytometric analysis. Cells were collected by 0.2% EDTA treatment and, after a wash in phosphate-buffered saline (PBS), 1×10^6 cells were reacted with first antibodies on ice for 30 min. The expression level of each protein was analyzed using a FACSCalibur (BD Biosciences). The antibodies used were mouse antihuman SSEA-4-phycoerythrin (PE) (clone MA813-7) (R&D Systems Inc., Minneapolis, MN), mouse antihuman Oct-4-PE (clone 240408) (R&D Systems Inc.), mouse antihuman CD11b-PE (clone ICRF44) (BD Biosciences), and mouse antinonhuman primate CD45-PE (clone D058-1283) (BD Biosciences). Before anti-Oct-4 antibody staining, cells were fixed and their plasma membranes were permeabilized using FIX & PERM (Caltag Laboratories, An-Der-Grub, Austria) according to the manufacturers guidance.

Immunostaining

The ES cells were seeded on Matrigel™-coated four-well-chamber slides (Nunc A/S, Roskilde, Denmark). After overnight culture, cells were washed by PBS and fixed with acetone/methanol solution (1:3) for 5 min at room temperature. The immunostaining procedure was performed as described elsewhere (Saeki et al., 2003) with first antibody reactions using a rabbit polyclonal antihuman Nanog antibody (ReproCELL Inc., Tokyo, Japan) followed by second antibody reactions using an Alexa Fluor® 488 goat antirabbit IgG (H+L) (Invitrogen Corp.).

Nitroblue tetrazolium (NBT) reduction assay for the respiratory burst activity

The floating cells were collected by mild centrifugation of culture supernatant. After a wash by PBS, the cells were resuspended in 1 mL of RPMI 1640 medium supplemented with 10% FBS containing 1 mg/mL nitroblue tetrazolium (NBT) (Nacalai Tesque Inc., Kyoto, Japan) and 100 ng/mL phorbol myristate acetate (Sigma Chemical Co.) for 30 min at 37°C. After a wash by PBS, cells were resuspended in 10 μL of PBS, which were dropped onto Matsunami Adhesive Silane (MAS)-coated slide glasses (Matsunami Glass Ind., Ltd. Osaka, Japan) and the formazan blue-black deposit-containing cells were observed under the light microscope (Olympus Optical Co. Ltd.).

Phagocytosis

The 100 μL of blue-dyed latex bead suspension (Sigma Chemical Co.) was pretreated by iso-volume of FBS at room temperature for 10 min, washed by PBS, and resuspended in 100 μL of DMEM medium. Two milliliters of the culture supernatant containing floating hematopoietic cells was mixed with 1 μL of FBS-treated latex bead suspension. After incubation at 37°C for 40 min, cells were washed with PBS, resuspended in 15 μL of PBS and dropped onto MAS-coated slide glasses (Matsunami Glass Ind. Ltd). Alternatively, 1 mL of culture supernatant containing floating hematopoietic cells was mixed with 10 μL of zymosan solution (1 mg/mL) and incubated at 37°C for 40 min. The cells were washed by PBS, resuspended in 10 μL of PBS, cytospin onto MAS-coated slide glasses using a cytospin apparatus (Cytospin2, SHANDON) and stained with Wright-Giemsa solution. Cells were observed under the light microscope (Olympus Optical Co. Ltd.).

Chemotaxis assay

Chemotaxis was assessed using Chemotaxel (3 μm pore; Kurabo Industries Ltd., Osaka, Japan), which was set on a 24-well dish. The lower chamber, a 24-well dish, was filled with 29 mL of HBSS and the upper chamber, a Chemotaxel cup, was filled with 50 mL of cynomolgus ES-derived hematocyte suspensions (2×10^6 cells/mL). As a chemoattractant, 100 nM formyl-methionyl-leucyl-phenylalanine (fMLP; Sigma Chemical Co.) was added to the lower chambers. After cells were incubated at 37°C for 2 h, filters at the bot-

TABLE 1. PRIMER SEQUENCES AND PRODUCT SIZES

		Sequence	*Product size*
Oct-4	F	GGACACCTGGCTTCGGATT	697
	R	TTCGCTTTCTCTTTCGGGC	
Nanog	F	GCTTGCCTTGCTTTGAAGCA	255
	R	TTCTTGACTGGGACCTTGTC	
Flk-1	F	CATATCTGTCCTGATGTGATATGTC	400
	R	CATAGCATGTCTTATAGTCATTGTTC	
GATA-2	F	GCACCTGTTGTGCAAATTGT	185
	R	CCCCTTTCTTGCTCTTCTTG	
CD10	F	CTGTGACAATGATCGCACTCTATG	586
	R	GATTCCAGTGCATTCATAGTAATCTC	
PU.1	F	CACAGCGAGTTCGAGAGCTT	194
	R	GATGGGTACTGGAGGCACAT	
NCF-1	F	TCTACCAGGTCCATTCG	436
	R	CTTCTATGCCCCCTGGTTCAG	
ε-globin	F	TGCATTTTACTGTGAGGAGA	450
	R	AAGAGAACTCAGTGGTACTT	
ζ-globin	F	TTCCTCAGCCACCCGCAGAC	223
	R	AGCAGGCAGTGGGACAGGAG	
γ-globin	F	AGACGCCATGGGTCATTTCACA	524
	R	GCCTATGGTTGAAAGCTCTGTAT	
α-globin	F	TGCACGCGCACAAGCTTCGG	152
	R	GCACGGTGCTCACAGAAGCCAG	
β-actin	F	GCAGGAGATGGCCACGGCGCC	280
	R	TCTCCTTCTGCATCCTGTCGGC	

The primer sequences and the product length of each gene are shown.